The Peak Index: Spirometry Metric for Airflow Obstruction Severity and Heterogeneity

Surya P. Bhatt[1,2*], Sandeep Bodduluri[1,2], Vrishank Raghav[3], Nirav R. Bhakta[4], Carla G. Wilson[5], Young-il Kim[1,6], Michael Eberlein[7], Frank C. Sciurba[8], MeiLan K. Han[9], Mark T. Dransfield[1,2], and Arie Nakhmani[10]; for the COPDGene Investigators

[1]Division of Pulmonary, Allergy, and Critical Care Medicine and Lung Health Center, [2]University of Alabama at Birmingham Lung Imaging Core, [6]Department of Preventive Medicine, and [10]Department of Electrical and Computer Engineering, University of Alabama at Birmingham, Birmingham, Alabama; [3]Department of Aerospace Engineering, Auburn University, Auburn, Alabama; [4]Division of Pulmonary, Critical Care, Allergy, and Sleep Medicine, University of California San Francisco, San Francisco, California; [5]Department of Biostatistics and Bioinformatics, National Jewish Health, Denver, Colorado; [7]Division of Pulmonary, Critical Care, and Occupational Medicine, University of Iowa Hospital, Iowa City, Iowa; [8]Division of Pulmonary, Allergy, and Critical Care Medicine, University of Pittsburgh, Pittsburgh, Pennsylvania; and [9]Division of Pulmonary and Critical Care Medicine, University of Michigan, Ann Arbor, Michigan

ORCID ID: 0000-0002-8418-4497 (S.P.B.).

Abstract

Rationale: Chronic obstructive pulmonary disease (COPD) is characterized by airflow limitation. Spirometry loops are not smooth curves and have undulations and peaks that likely reflect heterogeneity of airflow.

Objectives: To assess whether the Peak Index, the number of peaks adjusted for lung size, is associated with clinical outcomes.

Methods: We analyzed spirometry data of 9,584 participants enrolled in the COPDGene study and counted the number of peaks in the descending part of the expiratory flow–volume curve from the peak expiratory flow to end-expiration. We adjusted the peaks count for the volume of the lungs from peak expiratory flow to end-expiration to derive the Peak Index. Multivariable regression analyses were performed to test associations between the Peak Index and lung function, respiratory morbidity, structural lung disease on computed tomography (CT), forced expiratory volume in 1 second (FEV_1) decline, and mortality.

Results: The Peak Index progressively increased from Global Initiative for Chronic Obstructive Lung Disease stage 0 through 4 ($P < 0.001$). On multivariable analysis, the Peak Index was significantly associated with CT emphysema (adjusted $\beta = 0.906$; 95% confidence interval [CI], 0.789 to 1.023; $P < 0.001$) and small airways disease (adjusted $\beta = 1.367$; 95% CI, 1.188 to 1.545; $P < 0.001$), St. George's Respiratory Questionnaire score (adjusted $\beta = 1.075$; 95% CI, 0.807 to 1.342; $P < 0.001$), 6-minute-walk distance (adjusted $\beta = -1.993$; 95% CI, -3.481 to -0.506; $P < 0.001$), and FEV_1 change over time (adjusted $\beta = -1.604$; 95% CI, -2.691 to -0.516; $P = 0.004$), after adjustment for age, sex, race, body mass index, current smoking status, pack-years of smoking, and FEV_1. The Peak Index was also associated with the BODE (body mass index, airflow obstruction, dyspnea, and exercise capacity) index and mortality ($P < 0.001$).

Conclusions: The Peak Index is a spirometry metric that is associated with CT measures of lung disease, respiratory morbidity, lung function decline, and mortality.

Clinical trial registered with www.clinicaltrials.gov (NCT00608764).

Keywords: airflow obstruction; chronic obstructive pulmonary disease; spirometry; heterogeneity

(Received in original form November 21, 2018; accepted in final form March 12, 2019)

*S.P.B. is an Associate Editor for *AnnalsATS*. His participation complies with American Thoracic Society requirements for recusal from review and decisions for authored works.

Supported by National Institutes of Health (NIH) grant K23 HL133438 (S.P.B.) and the COPDGene study (NIH grants R01 HL089897 and R01 HL089856). The COPDGene project is also supported by the COPD Foundation through contributions made to an Industry Advisory Board comprising AstraZeneca, Boehringer Ingelheim, Novartis, Pfizer, Siemens, Sunovion, and GlaxoSmithKline.

Author Contributions: S.P.B. had full access to all of the data in the study and takes responsibility for the integrity of the data and accuracy of the analysis. S.P.B. and S.B. contributed to the conception and design of the study. S.P.B., C.G.W., F.C.S., M.K.H., and M.T.D. contributed to the acquisition of the data. S.P.B. and S.B. performed statistical analyses. S.P.B. drafted the manuscript. S.P.B., S.B., V.R., N.R.B., C.G.W., Y.-i.K., M.E., F.C.S., M.K.H., M.T.D., and A.N. contributed to revisions of the manuscript for critically important intellectual content. All of the authors approved this version of the manuscript to be published.

Correspondence and requests for reprints should be addressed to Surya P. Bhatt, M.D., University of Alabama at Birmingham, Division of Pulmonary, Allergy, and Critical Care Medicine, THT 422, 1720, 2nd Avenue South, Birmingham, AL 35294. E-mail: sbhatt@uabmc.edu.

This article has an online supplement, which is accessible from this issue's table of contents at www.atsjournals.org.

Ann Am Thorac Soc Vol 16, No 8, pp 982–989, Aug 2019

DOI: 10.1513/AnnalsATS.201811-812OC
Internet address: www.atsjournals.org

The diagnosis of chronic obstructive pulmonary disease (COPD) relies on demonstrating airflow obstruction using abnormalities in the flow–volume and volume–time curves on forced expiratory maneuvers (1). These "macro" abnormalities have proven useful for both diagnosis and the gradation of severity of obstructive airway disease (1). In addition, multiple studies have examined the utility of quantifying abnormalities in different portions of the expiratory curve with modest success in improvement in diagnosis and prognostication over the macro indices of airflow obstruction (2–8). Traditional models of airflow obstruction are based on a Starling resistor model, wherein airflow obstruction occurs when airflow-related intraluminal pressure losses in the airways equal the intrapleural pressure at the equal pressure point (EPP) (9). This model also suggests that there is a single choke point for the lung and that the EPP moves progressively distally with increasing airflow obstruction (9). However, the dynamics of airflow are likely much more complex, especially in those with disease.

Spirometry loops are not smooth curves and display a number of small undulations, with peaks and troughs (10). Although the reasons for these fluctuations are not clear, it is plausible that these are due to the heterogeneous contribution of airflow by different segments of the airway tree with their own choke points. During a forced exhalation maneuver, weakened conducting airways likely collapse partially or completely at different expiratory time points and, as intrapleural pressure decreases, contribute to airflow resulting in small peaks along the expiratory curve. Converting the spirometry curve to a Fourier transform and assessing the spectral patterns of these oscillations has shown promising results in differentiating obstructive patterns from normal (11). Assessment of heterogeneity of pathophysiological process in the lungs of patients with COPD has implications for clinical outcomes, but these assessments have traditionally required additional testing with lung imaging or with body plethysmography and lung diffusing capacity measurements (12–14). We hypothesized that a simple method of counting the number of peaks in the expiratory curve, adjusted for lung size, would reflect heterogeneity of airflow, be associated with clinically important outcomes in COPD, and also help stratify disease severity. We measured this index, termed the "Peak Index" in a large cohort of current and former smokers and tested the clinical and structural correlates of this new metric.

Methods

Study Population and Physiologic Assessments

We assessed expiratory spirometry curves of participants enrolled in a large multicenter cohort study, the COPDGene (Genetic Epidemiology of COPD) study (15). Participants were lifetime never smokers and current and former smokers between age 45 and 80 years. At the baseline visit, participants performed prebronchodilator and post-bronchodilator spirometry after administration of albuterol using the ndd Easy-One spirometer in accordance with the American Thoracic Society (ATS) criteria (16). All spirometry efforts had to meet at least grade 2 ATS standard (repeatable between 100 and 150 ml, and met ATS criteria) (17). For both pre- and post-bronchodilator spirometry, we selected the effort with the highest sum of forced expiratory volume in 1 second (FEV_1) and forced vital capacity (FVC). Post-bronchodilator values were used for testing associations with outcomes. COPD was defined by the ratio of FEV_1/FVC less than 0.70 and severity of disease stratified per the Global Initiative for Chronic Obstructive Lung Disease (GOLD) recommendations (1). We defined GOLD 0, per older recommendations, as those with FEV_1/FVC greater than or equal to 0.70 and FEV_1% predicted greater than or equal to 80%. Bronchodilator response (BDR) was defined per ATS criteria as 12% and 200-ml change in FEV_1 and/or FVC (17). We also categorized participants as FEV_1 responders and FVC responders if they had at least a 12% and 200-ml increase in FEV_1 and as FVC responders if they had at least a 12% and 200-ml increase in FVC.

Respiratory morbidity was assessed using the St. George's Respiratory Questionnaire (SGRQ); scores range from 0 to 100, with 100 being the worst quality of life (18). Dyspnea was measured using the modified Medical Research Council (mMRC) dyspnea score, and functional capacity was assessed by distance walked on the 6-minute-walk test (6MWD) (19). We calculated the BODE (body mass index [BMI], airflow obstruction, dyspnea, and exercise capacity) index to assess risk of mortality (20). Volumetric computed tomography (CT) scans were performed at end-inspiration (total lung capacity, TLC), and at end-expiration (functional residual capacity). Using density mask analyses, emphysema was quantified as the percentage of lung volume at TLC with attenuation less than −950 Hounsfield units and gas trapping as the percentage of lung volume at end-expiration with attenuation less than −856 Hounsfield units (15). Image registration and parametric response mapping (PRM) were used to match inspiratory and expiratory images voxel-to-voxel. We calculated the percentage of lung affected by emphysema (PRM^{emph}) and the percentage of functional small airways disease (PRM^{fSAD}) or nonemphysematous gas trapping, which is a measure of small airway disease (21). Pulmonary Workstation 2 (VIDA Diagnostics) was used to measure the wall area percentage of segmental airways as well as the Pi10 (square root of the wall area for a hypothetical airway with an internal perimeter of 10 mm) to quantify airway disease (15, 22). Participants returned at approximately 5 years and spirometry was repeated to measure annualized change in lung function.

Peaks Analysis

The flow–volume curves were recreated using raw data recorded every 30 ml for flow and every 60 milliseconds for volume measurements (details in the online supplement). The raw data points for each subject were treated as a data sequence, and local maxima (peaks) were identified. A local maximum flow (peak) was defined as a data point with value higher than its two neighboring data points in the series (i.e., at least a 60 ml/s increase from the prior lowest). All estimations were performed using the "findpeaks" function on MATLAB 9 (MathWorks Inc.). We counted the number of peaks in the descending part of the expiratory flow–volume curve from the peak expiratory flow to end-expiration. We adjusted the peaks count for the volume of the lungs from peak expiratory flow to end-expiration to derive the Peak Index. Figure 1 shows representative peaks analysis for

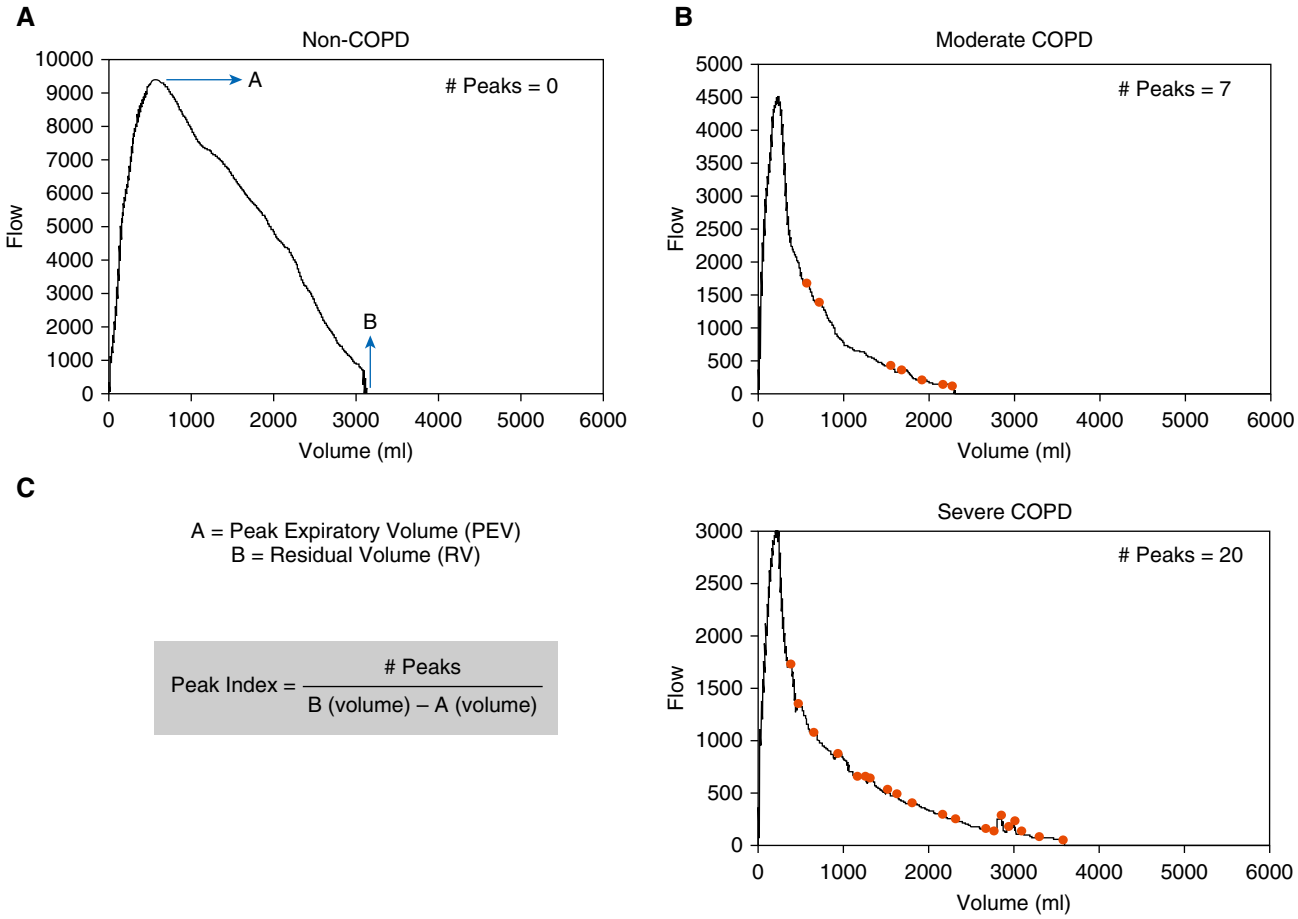

Figure 1. Representative peaks analysis for participants across a range of disease severity. (*A*) A 51-year-old white man with forced expiratory volume in 1 second (FEV_1)/forced vital capacity (FVC) of 0.89 and FEV_1% predicted of 84.5% has no peaks in the descending limb of the flow–volume loop. (*B*) A 70-year-old white woman with FEV_1/FVC of 0.64 and FEV_1% predicted of 69.6% has seven peaks. (*C*) A 54-year-old white man with FEV_1/FVC of 0.31 and FEV_1% predicted of 34.8% has 20 peaks. COPD = chronic obstructive pulmonary disease.

participants across a range of disease severity.

Statistical Analyses

Pearson and Spearman correlation tests were used to test relationships between the Peak Index and measures of lung function. Repeatability of measurement of the Peak Index over three efforts both pre- and post-bronchodilator was assessed by testing the intraclass correlation coefficients (ICC) with two-way mixed model and absolute agreement definition for interrater analysis. The accuracy of the Peak Index for the diagnosis of structural lung disease on CT was tested using receiver operating characteristic analyses. Generalized linear regression analyses were performed to test the associations between the Peak Index and outcomes including SGRQ and 6MWD, with adjustment for age, sex, race, BMI, current smoking status, pack-years of smoking, CT emphysema, and FEV_1. Similar models were created for the association between the Peak Index and FEV_1 change, with adjustment for age, sex, race, BMI, current smoking status, pack-years of smoking, and baseline FEV_1. Because of the ordinal nature of mMRC and BODE scores, we used Poisson regression analyses to test the association between the Peak Index and these outcomes, after adjustment for the above-mentioned variables, except for FEV_1 and BMI, as they are part of the BODE index.

Participants were divided into four groups on the basis of the distribution of the Peak Index, and survival rates were compared between these groups using Kaplan-Meier survival analysis with log-rank test. Using the lowest quartile of the Peak Index as the reference group, Cox proportional hazards were calculated for mortality for each higher quartile, with adjustment for age, sex, race, BMI, current smoking status, and pack-years of smoking. We considered a two-sided α of 0.05 as threshold for statistical significance. All analyses were performed using IBM SPSS Statistics for Windows, version 24.0 (IBM Corp.) and R statistical software (V 3.2).

Results

Subject Characteristics

Of the 10,300 participants enrolled in COPDGene, we had raw spirometry data points available for 9,896 individuals. For the primary analysis, we excluded 88 participants who were normal control subjects and 1,194 participants with preserved ratio with impaired spirometry

(23). In 224 participants, we were unable to calculate the number of peaks because of poor quality of the curves. We included data from 8,390 participants for the primary analysis and performed a secondary analysis with inclusion of subjects with preserved ratio with impaired spirometry (*see* Tables E1 and E2 in the online supplement). The baseline characteristics of these participants are shown in Table 1. Subjects encompassed the range of disease severity, had a mean age of 59.9 (standard deviation [SD] 9.1) years, and comprised 3,826 (45.6%) women and 2,620 (31.2%) African Americans. A total of 4,301 (51.3%) were current smokers, and the mean smoking burden was 44.3 (SD 25.1) pack-years. The mean SGRQ was 27.0 (SD 22.8). The median mMRC was 1.0 (interquartile range, 0–3.0), mean 6MWD was 417.6 (SD 121.0) m, and participants had a median BODE index of 1.0 (interquartile range, 0–3.0).

The absolute peak count ranged from 0 to 33 prebronchodilator with mean (SD) of 7.8 (5.4) and 0 to 37 on post-bronchodilator efforts with mean (SD) of 7.8 (5.6). After adjustment for lung size, the Peak Index ranged from 0 to 10.83, with a mean of 3.0 (1.99) prebronchodilator and ranged from 0 to 10.53 with a mean of 2.90 (1.97) post-bronchodilator. There was excellent repeatability for both prebronchodilator peak count (ICC, 0.910; 95% confidence interval [CI], 0.906 to 0.914; $P < 0.001$) and Peak Index (ICC, 0.901; 95% CI, 0.896 to 0.905; $P < 0.001$) and for post-bronchodilator peak count (ICC, 0.932; 95% CI, 0.929 to 0.935; $P < 0.001$) and Peak Index (ICC, 0.923; 95% CI, 0.920 to 0.926; $P < 0.001$). Post-bronchodilator values were used for all analyses.

Peak Index and Lung Function

Figure 2 shows that the Peak Index progressively increases from GOLD stages 0 through 4 (Jonckheere trend test $P < 0.001$). The Peak Index strongly correlated with both FEV_1/FVC and FEV_1% predicted ($r = -0.73$; $P < 0.001$ and $r = -0.67$; $P < 0.001$, respectively). On univariate regression, the Peak Index was significantly associated with FEV_1/FVC ($\beta = -0.062$; 95% CI, -0.063 to -0.061; $P < 0.001$). After adjustment for age, sex, race, BMI, pack-years of smoking, and current smoking status, the Peak Index remained significantly associated with FEV_1/FVC (adjusted $\beta = -0.054$; 95% CI, -0.056 to -0.053; $P < 0.001$). The Peak Index was also associated with FEV_1 after multivariable adjustment for the above-mentioned variables (adjusted $\beta = -0.259$; 95% CI, -0.266 to -0.252; $P < 0.001$).

Peak Index and Respiratory Morbidity

On univariate analysis, the Peak Index was significantly associated with SGRQ score ($\beta = 4.624$; 95% CI, 4.397 to 4.851; $P < 0.001$). This association remained significant after adjustment for age, sex, race, BMI, pack-years of smoking, current smoking status, and FEV_1 (adjusted $\beta = 1.075$; 95% CI, 0.807 to 1.342; $P < 0.001$). The Peak Index was also associated with the 6MWD on univariate ($\beta = -19.756$; 95% CI, -21.023 to -18.489; $P < 0.001$) and multivariable analysis (adjusted $\beta = -1.993$; 95% CI, -3.481 to -0.506; $P < 0.001$). The Peak Index was significantly associated with mMRC on univariate ($\beta = 0.179$; 95% CI, 0.171 to 0.187; $P < 0.001$) and multivariable analysis (adjusted $\beta = 0.028$; 95% CI, 0.016 to 0.040; $P < 0.001$). In addition, the Peak Index was also associated with the BODE index on both univariate ($\beta = 0.305$; 95% CI, 0.297 to 0.312; $P < 0.001$) and multivariable analyses adjusted for age, sex, race, pack-years of smoking, and active smoking status (adjusted $\beta = 0.294$; 95% CI, 0.286 to 0.302; $P < 0.001$).

Peak Index and Structural Lung Disease

PRM data were available in 6,759 subjects. On univariate analysis, the Peak Index was significantly associated with

Table 1. Baseline demographics

Parameters	COPD Severity Stages				
	GOLD 0 (*n = 4,145*)	GOLD 1 (*n = 749*)	GOLD 2 (*n = 1,825*)	GOLD 3 (*n = 1,102*)	GOLD 4 (*n = 569*)
Age, yr	56.7 (8.4)	61.9 (9.0)	62.6 (8.9)	64.4 (8.4)	63.9 (7.6)
Sex, female, *n* (%)	2,077 (47.1)	337 (42.4)	899 (46.5)	501 (42.7)	251 (41.2)
Race, African-American, *n* (%)	1,811 (41.1)	179 (22.5)	485 (25.1)	247 (21)	116 (19)
Body mass index, kg/m^2	28.9 (5.8)	27.0 (5.0)	28.7 (6.1)	28.1 (6.5)	25.5 (5.8)
Smoking, pack-years	37.1 (20.3)	44.9 (24.2)	50.7 (26.9)	54.8 (27.6)	56.5 (29.2)
Current smokers, *n* (%)	2,626 (59.6)	442 (55.7)	957 (49.5)	411 (35)	142 (23.3)
FEV_1, L	2.9 (0.7)	2.7 (0.7)	1.9 (0.5)	1.1 (0.3)	0.6 (0.2)
FEV_1% predicted	97.4 (11.4)	90.7 (8.7)	65.0 (8.6)	40.3 (5.7)	22.6 (4.9)
FVC, L	3.7 (0.9)	4.1 (1.0)	3.2 (0.9)	2.7 (0.8)	2.1 (0.7)
FVC % predicted	96.6 (11.8)	107.3 (12.0)	85.9 (12.6)	71.5 (13.3)	55.8 (13.6)
FEV_1/FVC	0.79 (0.05)	0.65 (0.04)	0.58 (0.08)	0.44 (0.09)	0.32 (0.07)
PRM emphysema, %*	0.6 (1.3)	2.4 (3.6)	5.0 (7.3)	14.5 (12.5)	25.5 (14.8)
PRM fSAD, %*	12.2 (10.4)	20.4 (11.5)	25.4 (12.2)	36.4 (11.3)	40.5 (9.5)
CT airway wall area thickness, WA%*	60.1 (2.8)	60.4 (2.6)	62.3 (2.9)	63.3 (2.9)	63.4 (2.8)
Pi10*	3.65 (0.11)	3.62 (0.11)	3.69 (0.13)	3.75 (0.14)	3.76 (0.14)

Definition of abbreviations: COPD = chronic obstructive pulmonary disease; CT = computed tomography; FEV_1 = forced expiratory volume in the first second; fSAD = functional small airway disease; FVC = forced vital capacity; GOLD = Global Initiative for Chronic Obstructive Lung Disease; Pi10 = square root of the wall area of a theoretical airway with internal perimeter of 10 mm; PRM = parametric response mapping; WA% = percent wall area of segmental bronchi.

All values are expressed as mean (standard deviation) unless specified otherwise.

*CT data available in 7,863 participants for WA%, 7,814 for Pi10, and 6,759 for PRM data.

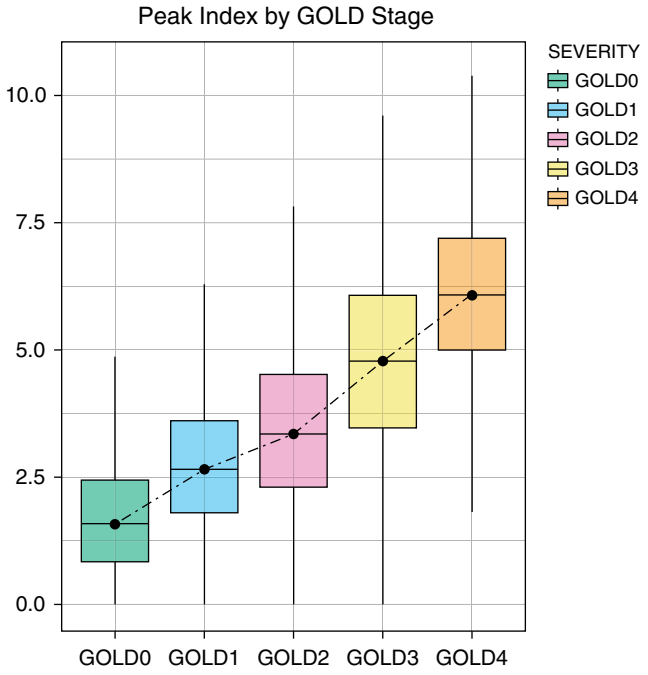

Figure 2. Mean Peak Index in participants by Global Initiative for Chronic Obstructive Lung Disease (GOLD) stage. Box plots show means and 95% confidence intervals.

PRM^{emph} (adjusted β = 2.753; 95% CI, 2.652–2.854; $P < 0.001$) and PRM^{fSAD} (adjusted β = 4.144; 95% CI, 3.994–4.294; $P < 0.001$). On multivariable analysis, the Peak Index was independently associated with PRM^{emph} (adjusted β = 0.906; 95% CI, 0.789–1.023; $P < 0.001$) and PRM^{fSAD} (adjusted β = 1.367; 95% CI, 1.188–1.545; $P < 0.001$), after adjustment for age, sex, race, BMI, current smoking status, pack-years of smoking, FEV_1, percentage wall area of segmental bronchi, and CT scanner type. The accuracy of the Peak Index in detecting 5% PRM^{emph} was excellent (C statistic, 0.85; 95% CI, 0.84–0.86; $P < 0.001$) and good for 10% PRM^{fSAD} (C statistic, 0.74; 95% CI, 0.73–0.75; $P < 0.001$).

Peak Index and FEV_1 Change

A total of 4,671 participants returned for follow-up spirometry at approximately 5 years. The mean FEV_1 change was −39.9 (SD 53.6) ml per year. After adjustment for age, race, sex, BMI, current smoking status, pack-years of smoking, and baseline FEV_1, there was a significant association between the Peak Index and annualized change in FEV_1 in milliliters per year (β = −1.604; 95% CI, −2.691 to −0.516; $P = 0.004$).

Peak Index and Bronchodilator Response

Participants with a positive bronchodilator response by any definition had a greater change in the absolute number of peaks and the Peak Index with the administration of bronchodilator. These changes were greater in magnitude in FVC responders (Table E3).

Peak Index and Mortality

We had mortality data on 7,332 participants followed for a median of 6.6 (range, 0.1–8.5) years. After adjustment for age, sex, race, BMI, current smoking status, and pack-years of smoking, the Peak Index was associated with all-cause mortality (adjusted hazard ratio [HR], 1.303; 95% CI, 1.265–1.343; $P < 0.001$). This association remained significant with adjustment for FEV_1 (adjusted HR, 1.064; 95% CI, 1.023–1.107; $P = 0.002$). We also divided the Peak Index into four quartiles (0–1.368, 1.369–2.514, 2.515–4.108, and ⩾4.109). Figure 3 shows Kaplan-Meier survival curves for the four groups. On Cox proportional hazards analysis, compared with the lowest quartile, the higher quartiles were associated with greater risk of all-cause mortality (adjusted HR, 1.10; 95% CI, 0.86–1.41; $P = 0.441$; adjusted HR, 1.50; 95% CI, 1.19–1.90; $P = 0.001$; and adjusted HR, 3.41; 95% CI, 2.75–4.23; $P < 0.001$, respectively), after adjustment for age, sex, race, BMI, current smoking status, and pack-years of smoking.

Discussion

In a cohort of current and former smokers, we showed that the number of peaks on the expiratory curve of the flow–volume loop, corrected for lung size, is associated with airflow obstruction and its severity, CT measures of emphysema and small airway disease, and respiratory morbidity. The Peak Index also predicts lung function decline and mortality.

The physiological basis of these peaks needs further investigation. The traditional model of airflow obstruction is simplistic and is based on the concept of an equal pressure point for the entire respiratory system, at which site the extraluminal intrapleural pressure equals the intraluminal airway pressure, and upstream of which is the choke point and the flow-limiting segment. With a forced exhalation maneuver, the EPP moves distally from the central cartilaginous airways with emptying of the lungs but remains in the well-supported conducting airways. Although the EPP is usually located in the cartilaginous airways in normal individuals, this point is reached more distally in the setting of increased intrapleural pressure or weakened airways, as seen in COPD. However, the dynamics of expiratory emptying of air from the lungs are likely much more complex, especially in those with disease. Either because of varying levels of increased airway resistance or because of poor elastic recoil and alveolar emptying, diseased lung regions do not empty uniformly (24). Warner and colleagues found that the lungs do not have a common regional flow–volume curve and that regional pressure–volume relationships are heterogeneous (25). Furthermore, anatomic heterogeneity might contribute; the Weibel model of symmetric daughter branches likely does not describe airway branching as accurately as the asymmetric Horsfield model (26). This asymmetry is greater in the smaller distal airway branches and is likely increased in diseases involving the small airways. Recent studies have also introduced other possibilities for airflow

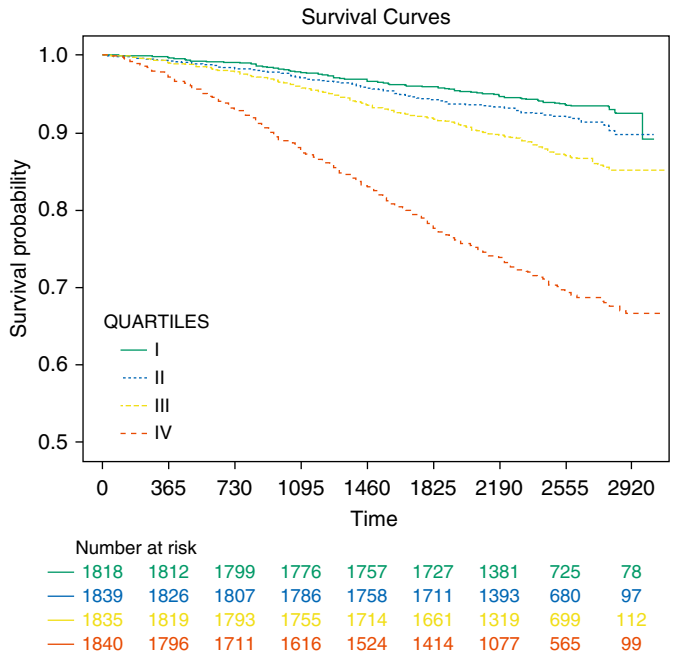

Figure 3. Kaplan-Meier survival curves for the four quartiles of Peak Index. After adjustment for age, sex, race, body mass index, current smoking status, and pack-years of smoking, compared with the lowest quartile (I), the higher quartiles were associated with greater risk of mortality (adjusted hazard ratio [HR], 1.10; 95% confidence interval [CI], 0.86–1.41; $P = 0.441$; adjusted HR, 1.50; 95% CI, 1.19–1.90; $P = 0.001$; and adjusted HR, 3.41; 95% CI, 2.75–4.23; $P < 0.001$, respectively).

limitation, including the wave-speed theory in which flow is limited at the site where the local air velocity equals the speed of pressure wave propagation (27, 28). The location of the choke point, depending on local dynamics and geometry, may vary irregularly along the conduit from the alveolus to the opening of the airway (27). Anogeianaki and colleagues used Fourier transform to analyze these "oscillations" using signal analysis and reported distinct patterns for those with and without airflow obstruction. These bumps may thus reflect a nonsmooth movement of the choke point from TLC to residual volume (11). These studies suggest that it is more plausible that individual lung segments have their own choke points, and the location of these points is very heterogeneous, depending on the dispersion of emphysema and airway disease. It is pertinent to note that these smaller peaks are distinct from the coarse oscillations observed sometimes in sleep apnea (29).

We show a schema (Figure 4) in a representative lung with heterogeneous airflow. During forced exhalation, some segments have partial or complete occlusion of the airways and no longer contribute to expiratory airflow. With progressive exhalation, the intrapleural pressure may decrease to a level sufficient to drop below the intraluminal pressure in these diseased segments, such that these airways now open again and contribute to overall airflow. With equilibration of pressure at successive airway branches, the consequent intermittent increase in flow results in peaks along the expiratory curve, reflecting the interdependence of regional expiratory flow. This concept is supported by multiple experiments done previously (30–32). With differential emptying of lung regions, the slowly emptying lung regions have a higher alveolar pressure (30). When airflow from two branches meets at airway branching points, the flow from the lung region with the higher driving pressure dominates (30). Thus, the peaks may reflect the degree of heterogeneity of involved airway segments. This differential contribution due to local choke points and differential alveolar emptying has also been likened to an electric circuit wherein there are multiple choke points that are not just parallel in arrangement but can also be serially arranged (31). Of note, these studies suggested that, despite the heterogeneity, airflow from regions that are not dynamically constricted tends to compensate for regions with flow limitation, such that the overall flow is near normal or normal. Thus, the parallel heterogeneity of flow at the local level remains hidden from the macro spirometry indices commonly used. In this study, we report a simple and easily calculable index on the basis of these principles, with strong associations with multiple clinical meaningful parameters. We acknowledge that alternative physiologic explanation for the peaks may exist. For instance, if pleural pressure decreases and intrathoracic gas becomes transiently decompressed, then lung volume and elastic recoil may increase, thus increasing driving and distending pressures and, in turn, maximal flow. With progressing expiration, the above mechanism can occur repeatedly in the same airway, thus causing jumps in the relocation of choke point not necessarily due to parallel heterogeneity. However, it is unlikely that such transient decompressions occur in a repeatable fashion between efforts in the same airway.

Although the mechanisms underlying a higher number of peaks and a greater Peak Index need more investigation, there are a number of clinical implications. The Peak Index can be readily calculated using existing data easily recorded by all modern spirometers. These data can help predict lung function decline and mortality, and this information on disease prognosis is additional to that offered by FEV_1 alone. We did find that participants with a positive bronchodilator response had a greater number of peaks prebronchodilator and a greater change in the peaks after the administration of a bronchodilator. The baseline number of peaks and the change with bronchodilator was greater in magnitude in FVC responders than in FEV_1 responders. It should be noted that an isolated FVC response is more strongly associated with emphysema and air trapping than an isolated FEV_1 response (33). An isolated FVC response may result from an imbalance between the longitudinal traction of airways and the radial traction of parenchymal tethering that is lower at higher lung volumes in subjects with emphysema, or because of compression of small airways by emphysema that is greater at higher than at lower lung volumes (34, 35). The change in peaks with bronchodilator

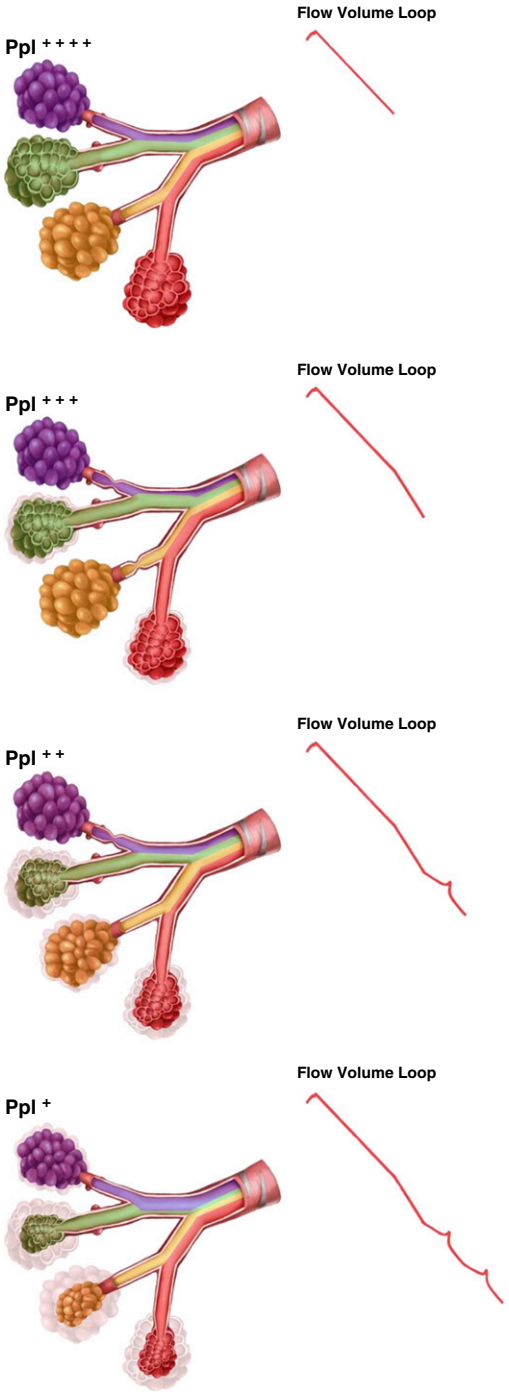

Figure 4. Schema showing choke points in airway segments in parallel and how these can potentially result in peaks on the expiratory limb of the flow–volume curve. Each segment is colored differently to show representative contribution from that airway segment to total airflow. The relative intrabronchial area occupied by a color represents the contribution to airflow from that airway segment. At the beginning of a forced exhalation maneuver, all segmental airways are open, and the colors are equally distributed. Initially, the intraalveolar pressures are very positive, and with exhalation this pressure gets progressively dissipated in the airways. With forced exhalation, the intrapleural pressure (Ppl) is initially high, and when the intrapleural pressure equals and exceeds the intrabronchial pressure in an airway branch, that airway collapses and there is a resultant decrease in the rate of decline of airflow. With progressive decrease in intrapleural pressure with exhalation, previously collapsed airway segments open up as their intrabronchial pressure rises above the intrapleural pressure.

is perhaps most in FVC-BDR, as at lower lung volumes the unopposed forces on airways lead to their narrowing, and thus they may be more sensitive to a decrease in airway smooth muscle tone with bronchodilator administration. This mechanism, however, has to be patchy in areas in which emphysema is predominant, such that peaks are induced because of regionally heterogeneous collapse, but overall exhaled volume increases, resulting in an increase in FVC.

Our study has several strengths. We analyzed data from a large multicenter cohort that included participants with a wide range of disease severity across a wide age range and had extensive CT phenotyping and stringent quality control of both spirometry and CT procedures. The cohort had a large number of African American individuals and women. The Peak Index has excellent repeatability over multiple efforts. The metric can be easily added to existing spirometry software, and no changes in testing preparation or procedures are necessary. In pulmonary function laboratories that use spirometers that sample flow and volume at different rates, the curves can be resampled at the same rate as in our study and peaks reported. The study also has a few limitations. We analyzed current and former smokers, and hence these results should be validated in other populations with varying disease risk; however, similar physiologic principles likely apply in non–smoking-related COPD. A saw-tooth pattern has been described in sleep apnea because of upper airway vibrations (29), and also in Parkinson's disease (36), but we did not have inspiratory curves available and could not test for this. However, the fluctuations in sleep apnea are coarser and not the fine fluctuations we reported. The fluctuations in Parkinson's disease are expected to be reproducible between spirometry efforts. The COPDGene study does not include detailed physiologic measurements, and hence the mechanisms underlying these observations need to be confirmed.

In summary, we report a new index of airflow heterogeneity and its severity that can be easily added to existing measures and can be used for disease diagnosis and prognostication. ■

Author disclosures are available with the text of this article at www.atsjournals.org.

Acknowledgment: The authors thank Ms. Jessica Surd for the artwork in Figure 4.

References

1 Vogelmeier CF, Criner GJ, Martinez FJ, Anzueto A, Barnes PJ, Bourbeau J, *et al*. Global strategy for the diagnosis, management, and prevention of chronic obstructive lung disease 2017 report: GOLD executive summary. *Am J Respir Crit Care Med* 2017;195:557–582.
2 Saltzman HP, Ciulla EM, Kuperman AS. The spirographic "kink": a sign of emphysema. *Chest* 1976;69:51–55.
3 Kapp MC, Schachter EN, Beck GJ, Maunder LR, Witek TJ Jr. The shape of the maximum expiratory flow volume curve. *Chest* 1988;94: 799–806.
4 O'Donnell CR, Rose RM. The flow-ratio index: an approach for measuring the influence of age and cigarette smoking on maximum expiratory flow-volume curve configuration. *Chest* 1990;98:643–646.
5 Topalovic M, Exadaktylos V, Peeters A, Coolen J, Dewever W, Hemeryck M, *et al*. Computer quantification of airway collapse on forced expiration to predict the presence of emphysema. *Respir Res* 2013;14:131.
6 Dominelli PB, Foster GE, Guenette JA, Haverkamp HC, Eves ND, Dominelli GS, *et al*. Quantifying the shape of the maximal expiratory flow-volume curve in mild COPD. *Respir Physiol Neurobiol* 2015;219: 30–35.
7 Li H, Liu C, Zhang Y, Xiao W. The concave shape of the forced expiratory flow-volume curve in 3 seconds is a practical surrogate of FEV_1/FVC for the diagnosis of airway limitation in inadequate spirometry. *Respir Care* 2017;62:363–369.
8 Wang W, Xie M, Dou S, Cui L, Xiao W. Computer quantification of "angle of collapse" on maximum expiratory flow volume curve for diagnosing asthma-COPD overlap syndrome. *Int J Chron Obstruct Pulmon Dis* 2016;11:3015–3022.
9 Mead J, Turner JM, Macklem PT, Little JB. Significance of the relationship between lung recoil and maximum expiratory flow. *J Appl Physiol* 1967;22:95–108.
10 Tien YK, Elliott EA, Mead J. Variability of the configuration of maximum expiratory flow-volume curves. *J Appl Physiol* 1979;46:565–570.
11 Anogeianaki A. Interpretation of spirometry through signal analysis. *Ups J Med Sci* 2007;112:313–334.
12 Hamedani H, Kadlecek S, Xin Y, Siddiqui S, Gatens H, Naji J, *et al*. A hybrid multibreath wash-in wash-out lung function quantification scheme in human subjects using hyperpolarized ^{3}He MRI for simultaneous assessment of specific ventilation, alveolar oxygen tension, oxygen uptake, and air trapping. *Magn Reson Med* 2017;78: 611–624.
13 Neder JA, O'Donnell CD, Cory J, Langer D, Ciavaglia CE, Ling Y, *et al*. Ventilation distribution heterogeneity at rest as a marker of exercise impairment in mild-to-advanced COPD. *COPD* 2015;12:249–256.
14 Davis C, Sheikh K, Pike D, Svenningsen S, McCormack DG, O'Donnell D, *et al*.; Canadian Respiratory Research Network. Ventilation heterogeneity in never-smokers and COPD: comparison of pulmonary functional magnetic resonance imaging with the poorly communicating fraction derived from plethysmography. *Acad Radiol* 2016;23:398–405.
15 Regan EA, Hokanson JE, Murphy JR, Make B, Lynch DA, Beaty TH, *et al*. Genetic epidemiology of COPD (COPDGene) study design. *COPD* 2010;7:32–43.
16 Pellegrino R, Viegi G, Brusasco V, Crapo RO, Burgos F, Casaburi R, *et al*. Interpretative strategies for lung function tests. *Eur Respir J* 2005;26: 948–968.
17 Miller MR, Hankinson J, Brusasco V, Burgos F, Casaburi R, Coates A, *et al*.; ATS/ERS Task Force. Standardisation of spirometry. *Eur Respir J* 2005;26:319–338.
18 Jones PW, Quirk FH, Baveystock CM, Littlejohns P. A self-complete measure of health status for chronic airflow limitation: the St. George's Respiratory Questionnaire. *Am Rev Respir Dis* 1992;145:1321–1327.
19 Mahler DA, Wells CK. Evaluation of clinical methods for rating dyspnea. *Chest* 1988;93:580–586.
20 Celli BR, Cote CG, Marin JM, Casanova C, Montes de Oca M, Mendez RA, *et al*. The body-mass index, airflow obstruction, dyspnea, and exercise capacity index in chronic obstructive pulmonary disease. *N Engl J Med* 2004;350:1005–1012.
21 Galbán CJ, Han MK, Boes JL, Chughtai KA, Meyer CR, Johnson TD, *et al*. Computed tomography-based biomarker provides unique signature for diagnosis of COPD phenotypes and disease progression. *Nat Med* 2012;18:1711–1715.
22 Sieren JP, Newell JD Jr, Barr RG, Bleecker ER, Burnette N, Carretta EE, *et al*.; SPIROMICS Research Group. SPIROMICS protocol for multicenter quantitative computed tomography to phenotype the lungs. *Am J Respir Crit Care Med* 2016;194:794–806.
23 Wan ES, Castaldi PJ, Cho MH, Hokanson JE, Regan EA, Make BJ, *et al*.; COPDGene Investigators. Epidemiology, genetics, and subtyping of preserved ratio impaired spirometry (PRISm) in COPDGene. *Respir Res* 2014;15:89.
24 Melissinos CG, Webster P, Tien YK, Mead J. Time dependence of maximum flow as an index of nonuniform emptying. *J Appl Physiol* 1979;47:1043–1050.
25 Warner DO, Hyatt RE, Rehder K. Inhomogeneity during deflation of excised canine lungs: II. Alveolar volumes. *J Appl Physiol (1985)* 1988; 65:1766–1774.
26 Horsfield K, Kemp W, Phillips S. An asymmetrical model of the airways of the dog lung. *J Appl Physiol* 1982;52:21–26.
27 Dawson SV, Elliott EA. Wave-speed limitation on expiratory flow-a unifying concept. *J Appl Physiol* 1977;43:498–515.
28 Pedersen OF, Butler JP. Expiratory flow limitation. *Compr Physiol* 2011; 1:1861–1882.
29 Sanders MH, Martin RJ, Pennock BE, Rogers RM. The detection of sleep apnea in the awake patient: the 'saw-tooth' sign. *JAMA* 1981;245: 2414–2418.
30 Wilson TA, Fredberg JJ, Rodarte JR, Hyatt RE. Interdependence of regional expiratory flow. *J Appl Physiol (1985)* 1985;59:1924–1928.
31 Solway J, Fredberg JJ, Ingram RH Jr, Pedersen OF, Drazen JM. Interdependent regional lung emptying during forced expiration: a transistor model. *J Appl Physiol (1985)* 1987;62:2013–2025.
32 McNamara JJ, Castile RG, Glass GM, Fredberg JJ. Heterogeneous lung emptying during forced expiration. *J Appl Physiol (1985)* 1987;63: 1648–1657.
33 Walker PP, Calverley PM. The volumetric response to bronchodilators in stable chronic obstructive pulmonary disease. *COPD* 2008;5:147–152.
34 Cerveri I, Pellegrino R, Dore R, Corsico A, Fulgoni P, van de Woestijne KP, *et al*. Mechanisms for isolated volume response to a bronchodilator in patients with COPD. *J Appl Physiol (1985)* 2000;88: 1989–1995.
35 Verbeken EK, Cauberghs M, Lauweryns JM, van de Woestijne KP. Anatomy of membranous bronchioles in normal, senile and emphysematous human lungs. *J Appl Physiol (1985)* 1994;77:1875–1884.
36 Schiffman PLA. A "saw-tooth" pattern in Parkinson's disease. *Chest* 1985;87:124–126.